Neurosci. Bull. February, 2022, 38(2):135–148
https://doi.org/10.1007/s12264-021-00773-x

www.neurosci.cn
www.springer.com/12264

ORIGINAL ARTICLE

Protein Kinase C Controls the Excitability of Cortical Pyramidal Neurons by Regulating Kv2.2 Channel Activity

Zhaoyang Li[1] · Wenhao Dong[1] · Xinyuan Zhang[1] · Jun-Mei Lu[1] · Yan-Ai Mei[1] · Changlong Hu[1]

Received: 20 January 2021 / Accepted: 11 May 2021 / Published online: 20 September 2021

Abstract The family of voltage-gated potassium Kv2 channels consists of the Kv2.1 and Kv2.2 subtypes. Kv2.1 is constitutively highly phosphorylated in neurons and its function relies on its phosphorylation state. Whether the function of Kv2.2 is also dependent on its phosphorylation state remains unknown. Here, we investigated whether Kv2.2 channels can be phosphorylated by protein kinase C (PKC) and examined the effects of PKC-induced phosphorylation on their activity and function. Activation of PKC inhibited Kv2.2 currents and altered their steady-state activation in HEK293 cells. Point mutations and specific antibodies against phosphorylated S481 or S488 demonstrated the importance of these residues for the PKC-dependent modulation of Kv2.2. In layer II pyramidal neurons in cortical slices, activation of PKC similarly regulated native Kv2.2 channels and simultaneously reduced the frequency of action potentials. In conclusion, this study provides the first evidence to our knowledge that PKC-induced phosphorylation of the Kv2.2 channel controls the excitability of cortical pyramidal neurons.

Keywords Kv2.2 · PKC · Phosphorylation · Pyramidal neurons · Excitability

✉ Zhaoyang Li
lzy@fudan.edu.cn

✉ Changlong Hu
clhu@fudan.edu.cn

[1] State Key Laboratory of Medical Neurobiology, Institutes of Brain Science and School of Life Sciences, Fudan University, Shanghai 200438, China

Introduction

Voltage-gated potassium Kv2 channels, consisting of Kv2.1 and Kv2.2 subtypes, play critical roles in the regulation of electrical excitability in neurons [1, 2]. Kv2.1 channels are widely expressed throughout the mammalian brain [1] and have been extensively studied. Because it is the major component of delayed rectifier K^+ currents in many neurons, Kv2.1 serves as a key regulator of neural excitability by controlling membrane repolarization and hyperpolarization [3, 4]. In addition to modulation of neuronal excitability, Kv2.1 has been implicated in Alzheimer's disease [5], traumatic brain injury [6], stroke [7], neuronal apoptosis [8], pain [9], diabetes [10, 11], and aging [12]. It is already clear that Kv2.1 channels are highly phosphorylated in the basal state in neurons, and their action depends on their phosphorylation state [13–15]. The dephosphorylation of Kv2.1 channels has been reported in various conditions such as ischemia, kainite-induced seizures, glutamate treatment, and CO_2 exposure; it leads to dynamic alteration of Kv2.1 channel localization and function and impacts the intrinsic excitability of neurons [14, 16, 17].

Compared with Kv2.1, much less is known about the dynamic modulation of Kv2.2 channels, even though Kv2.2 had been isolated in 1992 based on its homology to Kv2.1, which itself was cloned by Frech *et al.* in 1989 [18, 19]. The amino-acid sequences of Kv2.1 and Kv2.2 channels have ~62% identity, and the similarity is mainly located in the N-terminal and membrane-spanning domains (~92% identity). The C-terminal tail regions, in which the main Ser and Thr phosphorylation sites are located, are only 35% identical [18, 19]. Previous studies have shown that the Kv2.2 channel has a much lower phosphorylation level than the Kv2.1 channel (11 phosphorylation sites on

brain Kv2.2 *vs* 34 on Kv2.1) [20, 21]. Moreover, Kv2.2 is much less phosphorylated under basal conditions than Kv2.1 [22]. However, it remains largely unknown whether the differences between the amino-acid sequences of the carboxyl terminal tail regions and the phosphorylation status of Kv2.1 and Kv2.2 might lead to the utilization of a different mechanism controlling phosphorylation-dependent regulation of Kv2.2.

Although Kv2.2 mediates delayed rectifier K^+ currents [18, 23], this function is less clear relative to Kv2.1. Kv2.2 is expressed much less widely than Kv2.1; its expression is preferentially localized to the basal forebrain, the medial nucleus of the trapezoid body, and layers II and Va of the neocortex [22–24]. The function of Kv2.2 in maintaining high-frequency action potential (AP) firing has been recognized [23, 25] and has been implicated in sleep-wake cycles, noise-induced hearing loss, and the regulation of somatostatin release from pancreatic islets [26–28]. We have previously reported that inhibition of Kv2.2 in mouse cortical neurons by citalopram reduces the AP firing frequency [29]. Whether the function of Kv2.2 depends on its phosphorylation state in a manner similar to Kv2.1 needs to be further addressed.

Our previous study showed that Kv2.2 is modulated by resveratrol through the activation of PKC [30]. In the current study, we investigated whether Kv2.2 channels are phosphorylated by PKC and studied the effects of PKC phosphorylation on the activity and function of Kv2.2 channels in neurons of the neocortex.

Materials and Methods

Plasmids and Cell Transfection

RNA was extracted from rat cortical neurons using an RNeasy Kit (Qiagen, cat. no. 74106, Hilden, Germany), and reverse-transcribed using a reverse transcriptase from Thermo Fisher Scientific (cat. no. 18064064, Waltham, USA). The primers for Kv2.2 in PCR were: forward, 5'-CCGCTCGAGATGGCAGAAAAGGCACCTCCTGGCT TGA-3'; reverse, 5'-GGAATTCGCATGCTGGTCTCA CGAGTGGGGC-3. Rat Kv2.2 cDNA (NM_054000.2) was subcloned into pEGFPN1-expression vectors. To generate the plasmid constructs pEGFPN1/Kv2.2/S448A, /S451A, /S461A, /S481A, /S481D, /S488A, /S488D, /S481A/S488A, and /S481D/S488D, we mutated the cloned sequence of the mature form of Kv2.2 by substituting the serine residues at amino-acids 448, 451, 461, 481, and 488 with alanine and/or aspartic acid using a QuikChange Mutagenesis kit from Agilent (#210518, Santa Clara, USA) and ligated the fragment into pEGFPN1. The wild-type (WT) and mutant Kv2.2 channel constructs were verified by sequencing. Plasmids for rat WT and mutant Kv2.2 channels were transiently transfected into HEK293 cells using Lipofectamine from Thermo Fisher Scientific (cat. no. 11668019). The HEK293 cells were used for experiments 2 days after transfection.

Chemicals

The chemicals used in this study were all commercially available: phorbol 12'-myristate 13'-acetate (PMA, #8139, Sigma, St. Louis, USA), bryostatin-1 (BRY, # B7431, Sigma), and 4α-PMA (#P148, Sigma).

Patch-clamp Recordings

Whole-cell K^+ currents in HEK293 cells were recorded as previously reported [30], using an Axopatch 200B amplifier (Molecular Devices, San Jose, USA), digitally sampled at 10 kHz, and filtered at 1 kHz. Data were acquired using Clampex 10.7 software (Molecular Devices, San Jose, USA). The external bath solution contained (in mmol/L) 10 HEPES, 2.5 KCl, 1 $MgCl_2$, and 145 NaCl (pH 7.4). The internal solution contained (in mmol/L) 1 $CaCl_2$, 10 HEPES, 10 KCl, 1 $MgCl_2$, 2 ATP, 10 EGTA, and 135 K^+ gluconate (pH 7.3). Pipette resistances were 5–7 MΩ under these conditions. All recordings were performed at room temperature.

Western Blot and Immunoprecipitation

HEK293 cell lysates were prepared using a lysis buffer containing (in mmol/L) 2 EDTA, 50 NaF, 20 HEPES, 0.1 Na_3VO_4, 150 NaCl, 0.5% NP-40, 10% glycerol, pH 7.5 with protease inhibitor (#P8340, Sigma) and phosphatase inhibitor (#p5726, Sigma) cocktails on ice for 30 min. For cell surface expression experiments, the cell membrane proteins were isolated using the Membrane and Cytosol Protein Extraction Kit (Beyotime, #P0033, Shanghai, China). The protein samples with SDS loading buffer were boiled for 5 min, resolved using 10% sodium dodecyl sulfate-polyacrylamide gel electrophoresis (SDS PAGE) and then transferred to polyvinyldifluoride membranes (#1620177, Bio-Rad, Hercules, USA) at 90 V for 1 h. The membranes were blocked with 10% nonfat dry milk in Tris buffered saline with Tween-20 (TBST) and then incubated with primary antibodies overnight at 4°C [anti-phosphorylated PKC (pan), 1:1000, #9371, Cell Signaling Technology, Danvers, USA; anti-GAPDH, 1:1000; #AG109, Beyotime; anti-pPKC(α/β), 1:1000, #9375, Cell Signaling Technology; anti-pPKC(θ/δ), 1:1000, Cell Signaling Technology, #9376; anti-Na, K-ATPase, 1:1000, Cell Signaling Technology, #3010]. The membranes were washed 3 times in TBST, and then treated with horseradish peroxidase-

conjugated secondary antibodies (1:1000, Beyotime, #A0216 or A0208) at room temperature for 2 h. The signal was detected with enhanced chemiluminescence reagents and the ChemiDoc XRS+ imaging system from Bio-Rad.

For immunoprecipitation (IP), HEK293 cells transfected with WT and mutant Kv2.2 channels were homogenized in a lysis solution from Beyotime (#P0013C) supplemented with the same protease and phosphatase inhibitors as above. The lysate was centrifuged for 16 min at 21,000×g, and 75% of the supernatant from the lysate was incubated with antibody against Kv2.2 [pS481] or Kv2.2 [pS488] (1:50, Abmart, Shanghai, China) with gentle rotation overnight. The remaining 25% of the protein sample was used for loading. For precipitation, protein G magnetic beads were added to the protein samples, mixed, and incubated for 3 h at 4°C. The IP samples were harvested by eluting with pH 2.0 100 mmol/L glycine, followed by neutralization with pH 7.4 PBS. The samples were used for Western blots with the Kv2.2 antibody (#75-015, NeuroMab, Davis, USA).

Brain Slice Preparation and Action Potential Recordings

Adult female C57/LB mice (3–4 weeks old) were purchased from Shanghai SLAC Laboratory Animal Co., Ltd, Shanghai, China. To minimize suffering, mice were deeply anesthetized (50 mg/kg pentobarbital sodium, intraperitoneal) before rapid decapitation. The brains were coronally sectioned (200 μm, bregma 3.6–2.5 mm; VT1200S; Leica, Wetzlar, Germany) in ice-cold buffer solution containing (in mmol/L): 26 $NaHCO_3$, 3 KCl, 5 $MgCl_2$, 220 sucrose, 10 glucose, 1 $CaCl_2$, and 1.25 NaH_2PO_4 bubbled with 95% O_2/5% CO_2. The slices were put into an incubation solution containing (in mmol/L): 1.5 $MgSO_4$, 2.5 KCl, 125 NaCl, 1 NaH_2PO_4, 2.5 $CaCl_2$, 11 glucose, and 26.2 $NaHCO_3$, 305 mOsm/L at 35°C with 5% CO_2 for 1 h, and then kept at room temperature.

The APs of pyramidal neurons in layer II of the cortical slices were recorded in current-clamp mode. Under the microscope, layers I and II/III in the slices are very easy to distinguish. The pyramidal neurons adjacent to layer I (within ~150 μm) were chosen for recording. The external solution for AP recordings contained (in mmol/L) 2.5 KCl, 140 NaCl, 10 HEPES, and 1 $MgCl_2$, pH 7.4 adjusted with NaOH; or 2.5 KCl, 119 NaCl, 3 $MgSO_4$, 1 Na_2HPO_4, 11 glucose, 1 $CaCl_2$, and 26.2 $NaHCO_3$. The pipette solution for AP recordings contained (in mmol/L) 10 HEPES, 150 K^+ gluconate, 8 NaCl, 0.4 EGTA, 0.1 GTP·Na_3, and 2 ATP·Mg, pH 7.3 adjusted by KOH. All recordings were performed at room temperature.

The protocol for the mouse brain experiments was approved by the Ethics Committee of Animal Experimentation at Fudan University (permit # 20090614-001).

Data Analysis

Statistical analysis consisting of unpaired or paired Student's *t*-tests was used to compare two samples, as appropriate. The Shapiro–Wilk test was used to verify the normal distribution of data. For more than two groups, ANOVA (analysis of variance) with Bonferroni's *post hoc* test was used. Data are given as the mean ± SEM; *n* indicates the number of cells tested, or independent experiments of Western blot. $P < 0.05$ was considered statistically significant.

Results

Activation of PKC Modifies Kv2.2 Channels Over-expressed in HEK293 Cells

We first used PMA, the typical PKC activator, to assess the effect of PKC activation in HEK293 cells. PMA activated PKC in a concentration-dependent manner and 1 μmol/L produced maximal activation (Fig. 1A, left). The effect of PMA on PKC activation occurred quickly and reached the maximum in ~10 min (Fig. 1A, right). We thus used 1 μmol/L PMA to investigate the effect of PKC activation on Kv2.2 channels over-expressed in HEK293 cells. Whole-cell Kv2.2 currents were evoked by a 160-ms step (−80 to +60 mV) from a holding potential of −80 mV. PMA significantly decreased the amplitude of Kv2.2 currents by 41.8% ± 4.3% ($n = 5$, $P = 0.0006$) and was reversible (Fig. 1B).

Since previous studies of Kv2.1 indicated that phosphorylation- or dephosphorylation-induced modification of the K^+ channel by PKA mainly affected its activation characteristics [13, 14], we investigated whether PMA modulated the steady-state activation kinetics of the Kv2.2 current using corresponding voltage protocols. The Kv2.2 currents were elicited by 200-ms steps (−60 to +60 mV in 10-mV increments) from a holding potential of −80 mV at 10-s intervals (Fig. 1C, left). The current–voltage relationship (I–V curve) showed that PMA significantly inhibited Kv2.2 channels at all testing potentials that were more positive than −10 mV (Fig. 1C, right). The steady-state activation (G–V curve) of Kv2.2 currents was obtained by plotting normalized Kv2.2 conductance (G/G_{max}) as a function of the command voltage (Fig. 1D); the conductance of Kv2.2 was analyzed using the equation $G_K = I/(V_m - V_{rev})$, where V_{rev} is the reversal potential for the Kv2.2 current, and V_m is the membrane potential. The half-

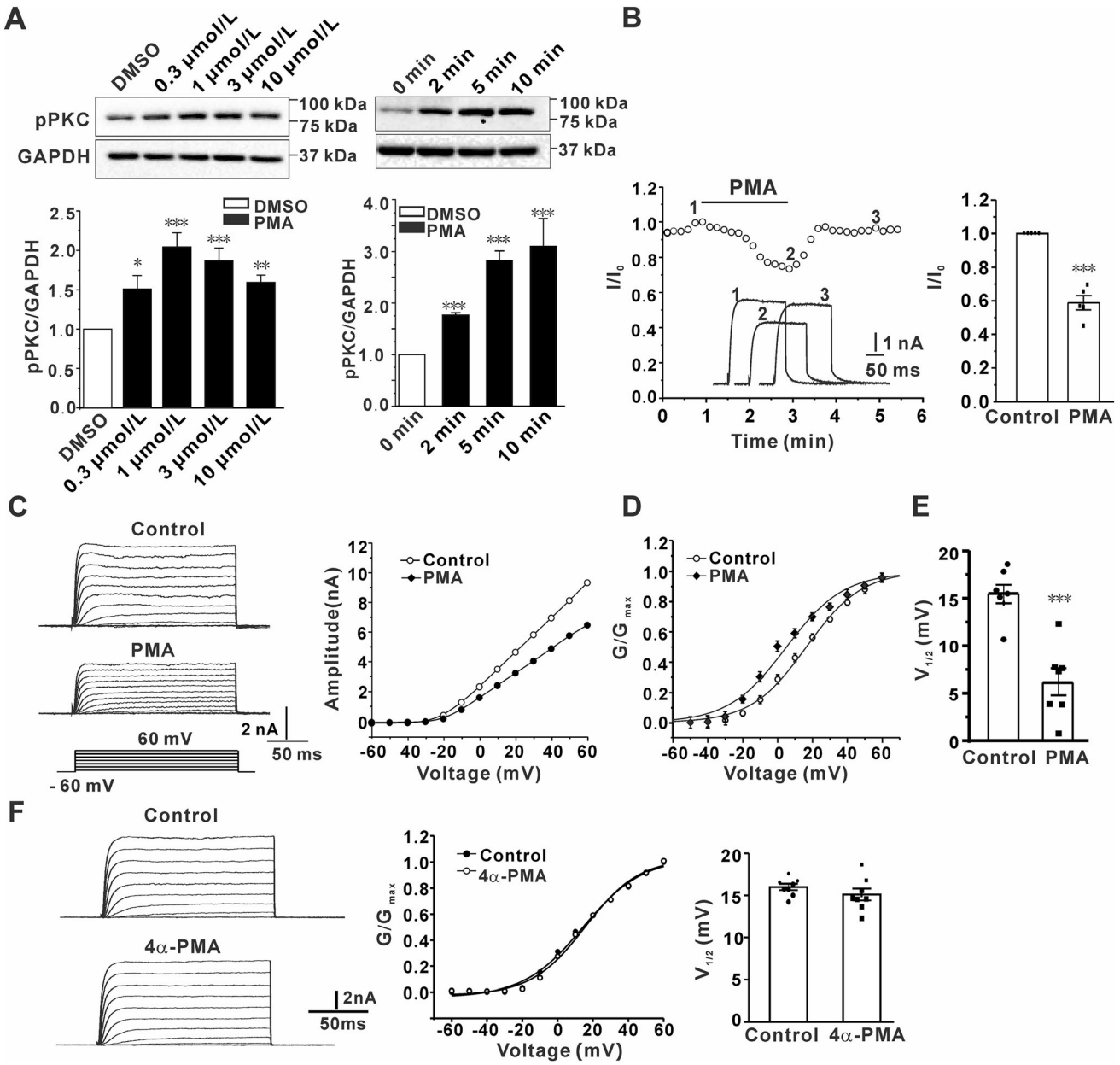

Fig. 1 PMA activates PKC and modifies Kv2.2 channels overexpressed in HEK293 cells. **A** Representative Western blots and statistical analysis showing that PMA activates PKC in a concentration- and time-dependent manner (3 independent experiments; $^{*}P$ <0.05, $^{**}P$ <0.01, $^{***}P$ <0.001 *vs* corresponding control by one-way ANOVA). **B** Representative time course of the changes in Kv2.2 current amplitude and statistical analysis showing the effect of PMA on current amplitude of Kv2.2 channels. Inset: superimposed Kv2.2 traces from the initial control levels (after establishment of the whole-cell configuration) and after external infusion of PMA. Time points 1, 2, and 3 denoted on the curves correspond to the superimposed Kv2.2 traces in the inset. **C** Representative current traces and voltage-dependent activation curves in the absence or presence of PMA. **D** Conductance–voltage relationship curve (G–V curve) obtained by plotting normalized conductance as a function of the command potential in the absence or presence of PMA; data points are fitted using the Boltzmann function. **E** Statistical analysis showing the effect of PMA on the half-activation potential ($V_{1/2}$) of Kv2.2 channels. **F** 4α-PMA, the inactive form of PMA, does not alter the Kv2.2 current. Data are reported as the mean ± SEM from 5–10 cells. $^{***}P$ <0.001 *vs* corresponding control by paired *t*-test.

activation potential ($V_{1/2}$) of Kv2.2 was obtained by fitting the Kv2.2 conductance with the Boltzmann function, $G/G_{max} = A2 + (A1-A2)/\{1 + \exp[(V_m - V_{1/2})/\text{slope factor}]\}$. As shown in Fig. 1, the $V_{1/2}$ was shifted from 15.4 ± 1.3 mV to 6.2 ± 1.7 mV in the presence of PMA (n = 10, $P = 7.4 \times 10^{-7}$; Fig. 1E), hyperpolarizing the activation curve by 9.3 ± 1.0 mV. In contrast, 4α-PMA, the inactive form of PMA, did not alter the activation kinetics of Kv2.2 currents (Fig. 1F).

In order to confirm the PKC effect on Kv2.2 channels, we tested another PKC activator, BRY. Similar to PMA, BRY significantly activated PKC in a time- and concentration-dependent manner, and reached a maximal stimulatory effect at 1 μmol/L (Fig. 2A); therefore, we used 1 μmol/L for the subsequent experiments. Whole-cell Kv2.2 currents indicated that 1 μmol/L BRY had a similar inhibitory effect on Kv2.2 currents and reversibly inhibited the amplitude of Kv2.2 currents by 32.6% ± 1.7% (n = 13, $P = 2.8 \times 10^{-10}$; Fig. 2B). Moreover, BRY similarly shifted the steady-state activation curve of Kv2.2 current towards a more negative voltage (Fig. 2C). In the presence of 1 μmol/L BRY, $V_{1/2}$ was shifted from 19.5 ± 1.0 mV of control to 11.4 ± 1.9 mV, hyperpolarizing the activation curve by 8.0 ± 1.8 mV (n = 10, P = 0.0013; Fig. 2D). The above data demonstrated that activation of PKC inhibited Kv2.2 current amplitude and modified the steady-state activation kinetics.

Both PMA and BRY can activate several PKC subtypes including PKCα, PKCβ, PKCδ, and PKCθ [31, 32]. We found that PMA and BRY mainly activated the PKCδ subtype in HEK293 cells (Fig. 3).

PKC Regulates Kv2.2 Channels Through S481 and S488 Sites

According to previous phospho-proteomic studies [33–37] and the PhosphoSitePlus index (https://www.phosphosite.org/homeAction.action), there are five possible phosphorylation sites (S448, S451, S461, S481, and S488; Fig. 4A) near the proxC sequence, which is the special proximal carboxyl terminal sequence in Kv2.2. We thus tested which site is more important for the PKC regulation of Kv2.2 channels by changing the serine amino-acid at each site to alanine. As shown in Fig. 4, the point mutations S448A, S451A, and S461A did not change the PMA-induced shift of the G–V curve for Kv2.2; the hyperpolarizing shifts were 12.5 ± 2.4 mV (n = 5, P = 0.0068), 8.2 ± 0.5 mV (n = 7, $P = 4.2 \times 10^{-6}$), and 13.9 ± 1.6 mV (n = 7, $P = 1.2 \times 10^{-4}$), respectively (Fig. 4B, C), and the inhibition of Kv2.2 current amplitude was 34.3% ± 3.7% (n = 7, P <0.001 $P = 9.0 \times 10^{-5}$), 38.0% ± 4.5% (n = 7, $P = 1.4 \times 10^{-4}$), and 28.9% ± 1.8% (n = 8, $P = 2.1 \times 10^{-4}$), respectively (Fig. 4D). In contrast, the effect of the point mutations S481A and S488A was to decrease the shift in the PMA-induced $V_{1/2}$ curve to 4.2 ± 0.9 mV (n = 9, P =

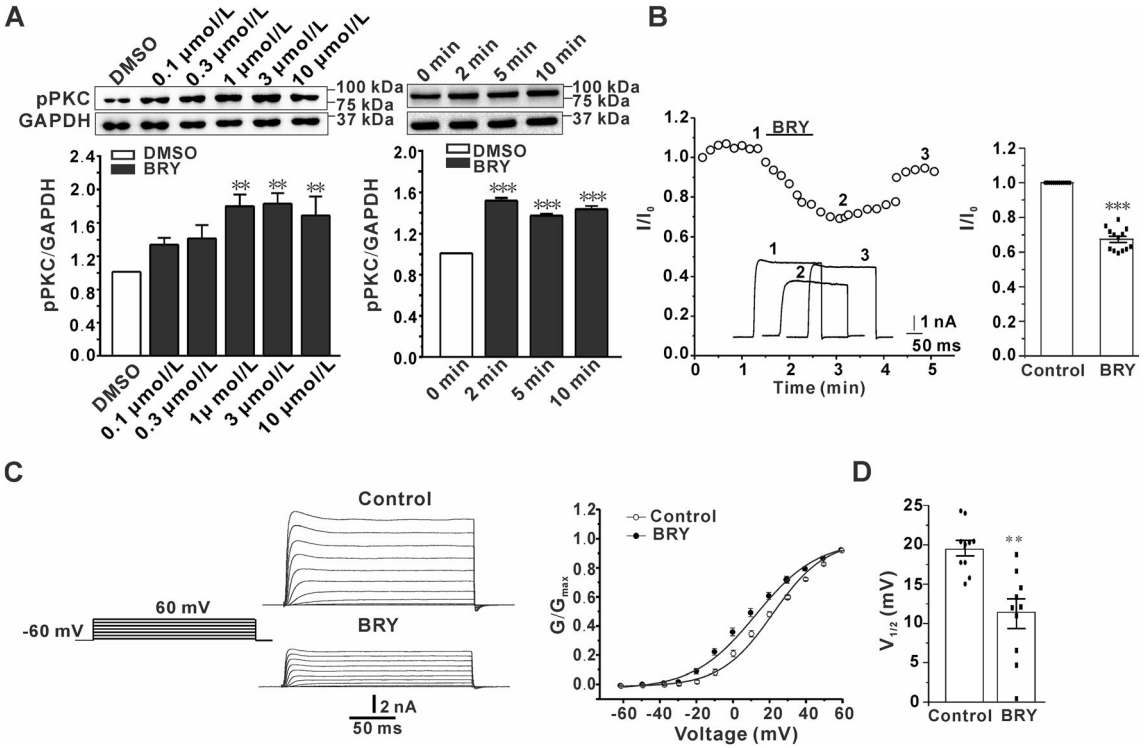

Fig. 2 Bryostatin-1 (BRY) activates PKC and modifies Kv2.2 channels over-expressed in HEK293 cells. **A** Representative Western blots and statistical analysis showing that BRY activates PKC in HEK293 cells in a concentration- and time-dependent manner (3 independent experiments; $^{**}P$ <0.01, $^{***}P$ <0.001 *vs* corresponding control by one-way ANOVA). **B** Representative time course of the changes in Kv2.2 amplitude and statistical analysis showing the effect of BRY on current amplitude of Kv2.2 channels. Inset as in **B**. **C** Representative current traces in the absence or presence of BRY and the G–V curve showing the effect of BRY on the voltage-dependent activation of Kv2.2 channels. **D** Statistical analysis showing the effect of BRY on the $V_{1/2}$ of Kv2.2 channels. Data are reported as the mean ± SEM from 10–13 cells. $^{**}P$ <0.01, $^{***}P$ <0.001 *vs* corresponding control by paired *t*-test.

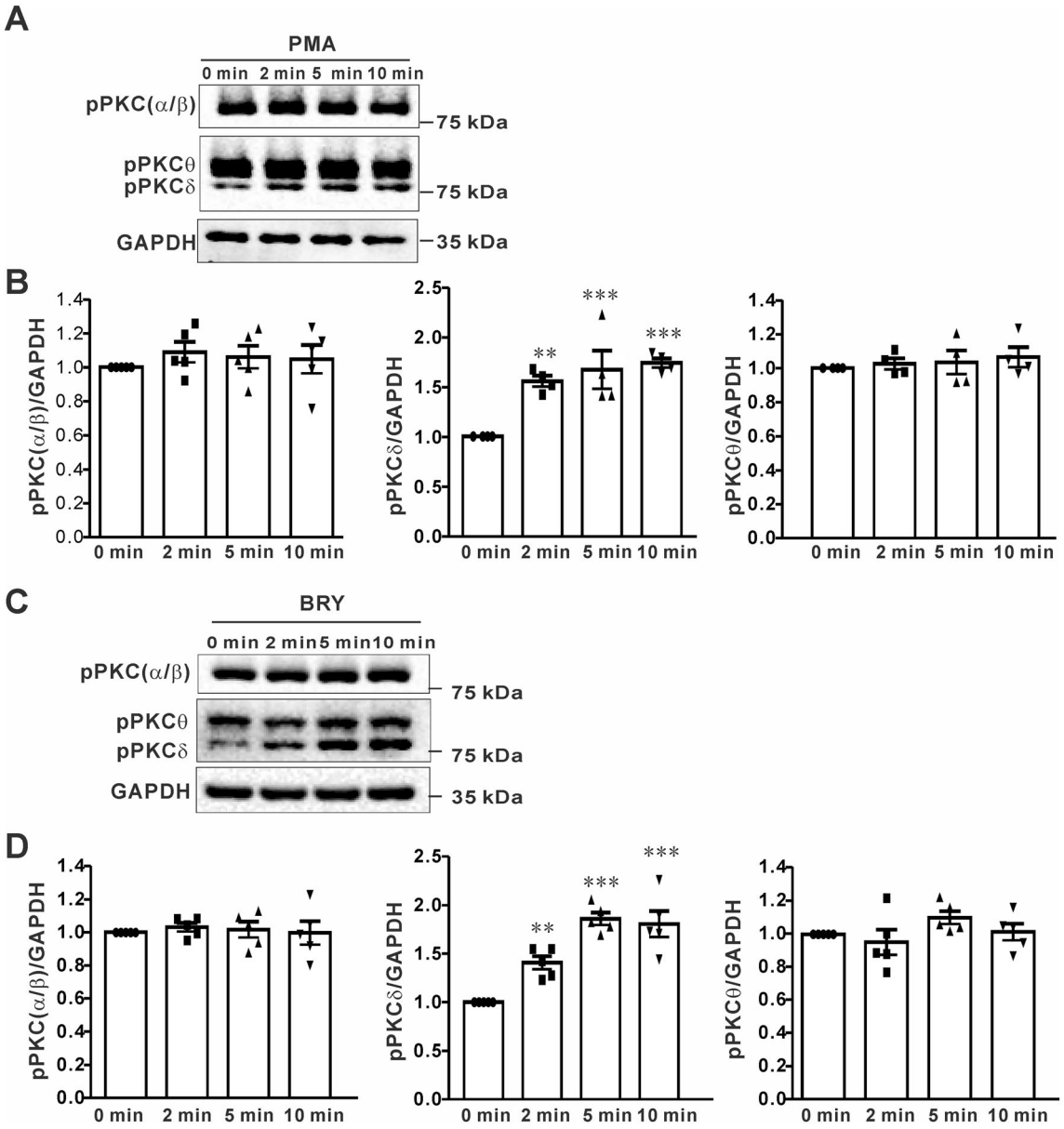

Fig. 3 PMA and BRY mainly activate the PKCδ subtype in HEK293 cells. **A**, **B** Representative Western blots and statistical analysis showing the effects of PMA on different PKC subtypes. **C**, **D** Representative Western blots (**C**) and statistical analysis (**D**) showing the effects of BRY on different PKC subtypes in HEK293 cells. $^{**}P$ <0.01, $^{***}P$ <0.001 *vs* corresponding control.

0.0012) and 4.0 ± 1.2 mV (n = 7, P = 0.0063), respectively (Fig. 5A, B). The S481A and S488A mutations reduced the PMA inhibitory effect on Kv2.2 current amplitude to 16.4% ± 1.2% (n = 10, $P = 2.0 \times 10^{-7}$) and 13.6% ± 3.4% (n = 10, P = 0.0029; Fig. 5C), respectively. We then tested whether these sites could account for the whole effect of PMA on Kv2.2 channels by making S481A/S488A double mutants. The results showed that this mutation reduced the extent of the PMA-induced $V_{1/2}$ shift to 1.4 ± 1.0 mV (n = 5, P = 0.2444 *vs* control; Fig. 5A, B) and lowered the inhibition caused by PMA on the Kv2.2 current amplitude to 1.9% ± 1.6% (n = 9, P = 0.2563; Fig. 5C), suggesting that both S481 and S488 sites are important for the regulation of Kv2.2 channels by PKC.

In addition to the serine-to-alanine mutations, we also made S481D or S488D single mutations and the S481D/S488D double mutation to address whether the serine-to-aspartic acid mutation could mimic the PMA-induced effect of phosphorylation on Kv2.2 channels. Both K_V2.2 current density and the $V_{1/2}$ of the activation curve were measured. As expected, both the S481D and S488D mutations produced a small shift in $V_{1/2}$ from 17.3 ± 0.4 mV in WT Kv2.2 to 14.8 ± 0.7 mV (n = 17, P = 0.0336 and 15.8 ± 1.3 mV (n = 15, P = 0.1891) in the S481D and

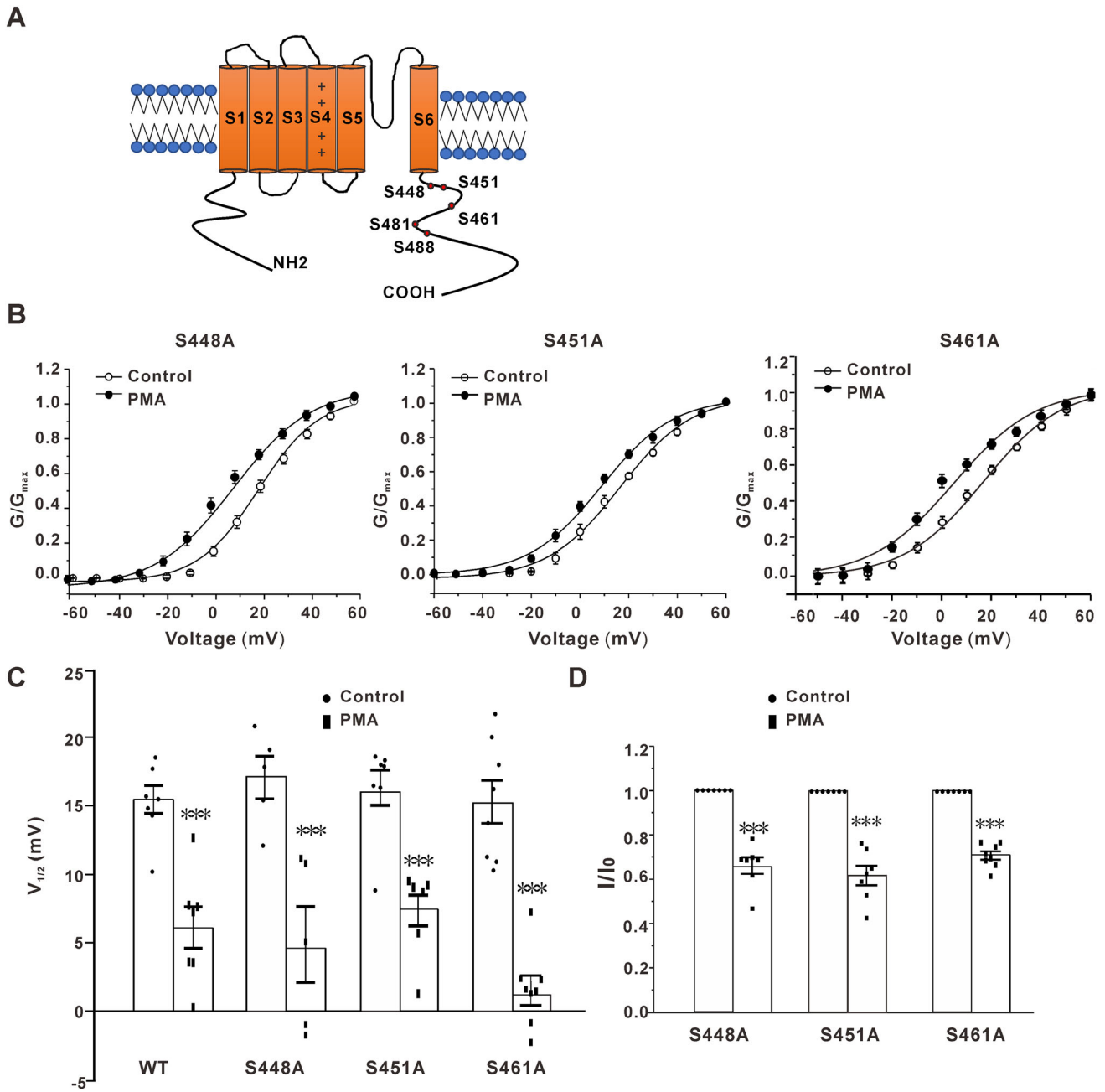

Fig. 4 Effect of PMA on Kv2.2 channels with point mutations S448A, S451A, or S461A in HEK293 cells. **A** Schematic structural models of Kv2.2 channels showing the locations of S448, S451, S461A, S481, and S488 residues. **B** G–V curves of Kv2.2 channels with S448A, S451A, or S461A point mutations in the absence or presence of PMA. **C** Statistical analysis showing the effect of PMA on $V_{1/2}$ of Kv2.2 channels with S448A, S451A, or S461A point mutations. **D** Statistical analysis showing the effect of PMA on current amplitude of Kv2.2 channels with point mutations S448A, S451A, or S461A. Data are reported as the mean ± SEM from 7–10 cells. ***P <0.001 *vs* corresponding control by paired *t*-test.

S488D mutations, respectively, hyperpolarizing the shifts of the steady-state activation curves by 2.5 ± 0.7 mV and 1.6 ± 1.3 mV for the S481D and S488D mutations, respectively (Fig. 6A, B). Kv2.2 current density after S481D or S488D mutation significantly decreased from 324.5 ± 25.4 pA/pF in the WT Kv2.2 channel to 194.6 ± 21.8 pA/pF (n = 17, $P = 1.8 \times 10^{-4}$) and 194.3 ± 18.2 pA/pF (n = 23, $P = 4.9 \times 10^{-5}$), respectively (Fig. 6C). S481D/S488D double mutations significantly hyperpolarized the shift in the steady-state activation curve by 6.4 ± 1.1 mV (n = 16, $P = 4.5 \times 10^{-6}$) and reduced the Kv2.2 current amplitude by 49%, similar to the effect of PMA on the WT channel. The PMA-mimicking effect of S481D/S488D was

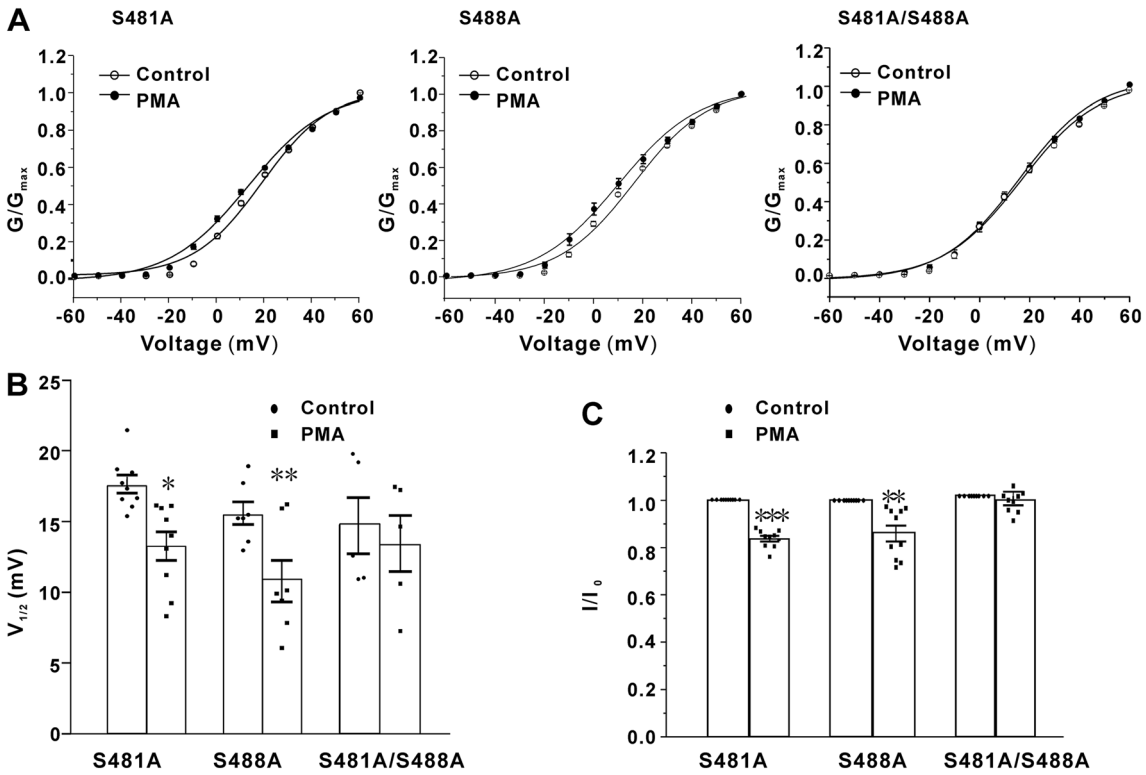

Fig. 5 Effect of PMA on Kv2.2 channels with S481A, S488A, or double point mutations in HEK293 cells. **A** G–V curves of mutated Kv2.2 channels in the absence or presence of PMA. **B** Statistical analysis showing the effect of PMA on $V_{1/2}$ of mutated Kv2.2 channels. **C** Statistical analysis showing the effect of PMA on current amplitude of mutated Kv2.2 channels. Data are reported as the mean ± SEM from 7–12 cells. **P* <0.05, ***P* <0.01, ****P* <0.001 *vs* corresponding control by *t*-test.

significantly greater than that of the S481D or S488D mutation alone (Fig. 6A–C).

We then investigated whether S481 and S488 were really phosphorylated by PMA by using specific antibodies against phosphorylated S481 or S488. As shown in Fig.7, 1 μmol/L PMA increased the phosphorylation of S481 by 1.8-fold (n = 3, P = 0.0012), but the phosphorylation state-specific antibody against S481 did not recognize the S481A mutant of Kv2.2 (Fig. 7A). Furthermore, 1 μmol/L PMA significantly increased the phosphorylation of S488 by 2.9-fold (n = 5, P = 0.02), but the phosphorylation state-specific antibody against S481 did not recognize the S488A mutant of Kv2.2 (Fig. 7B). The above data thus demonstrated that the activation of PKC, which inhibited Kv2.2 current amplitude and modified the activation properties of Kv2.2 channels, is associated with the phosphorylation of the S481/S488 site in Kv2.2 channels.

The cell surface expression of Kv2 channels is altered by phosphorylation [38]. Therefore, we tested whether the inhibitory effect of PKC on Kv2.2 channels is *via* regulating their surface expression. As shown in Fig. 8, 1 μmol/L PMA did not alter the surface expression of Kv2.2 channels (n = 6, P >0.05).

PKC Reduces Membrane Excitability of Cortical Pyramidal Neurons *via* Kv2.2 Channels

Kv2.2 has been shown to be preferentially expressed in layers II and Va of the cortex, so we next investigated the physiological action of PKC phosphorylation of Kv2.2 channels in pyramidal neurons from cortical layer II of mice. As shown in Fig. 9, perfusion of mouse brain slices with 1 μmol/L PMA significantly reduced the rectified outward K^+ current (I_K) of neocortical layer II pyramidal neurons by 32.5% ± 1.9% (n = 9, P = 1.3 × 10^{-7}; Fig. 9A), and hyperpolarized the shift in the G–V curve of I_K by 12.5 ± 2.2 mV (n = 10, P = 2.9 × 10^{-4}; Fig. 9B), a result which was similar to that from Kv2.2 channels over-expressed in HEK293 cells. Since Kv2.2 is known to play key roles in controlling the excitability of pyramidal neurons [25, 39], we investigated the effect of PMA on neuronal excitability by recording the APs evoked by a 1-s 150-pA current from a holding potential of –80 mV. As shown in Fig. 7, 1 μmol/L PMA significantly decreased the AP firing frequency by 39.2% ± 5.3% (n = 6, P = 9.2 × 10^{-4}; Fig. 9C), while no significant alteration was found in the resting membrane potential of cortical pyramidal neurons after applying PMA (n = 10, P = 0.2789;

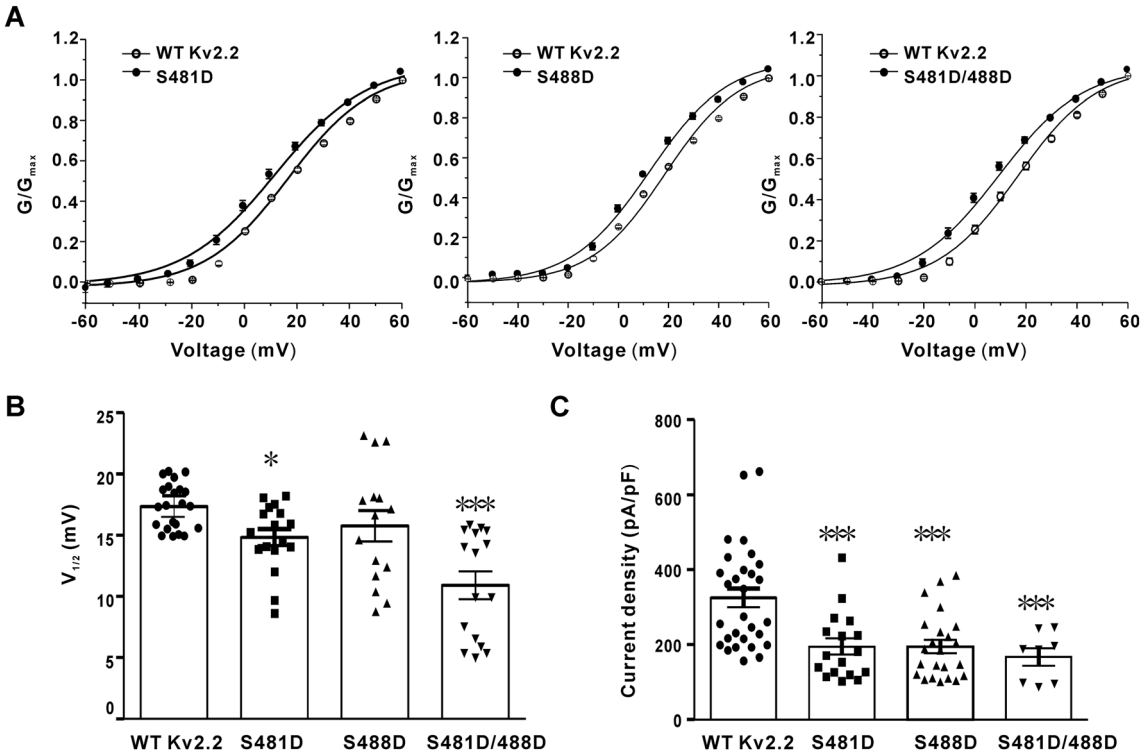

Fig. 6 Effect of S481D, S488D, or double (S481D/S488D) point mutations on Kv2.2 channels in HEK293 cells. **A** G–V curves of WT and mutated Kv2.2 channels. **B** Statistical analysis showing the effect of the mutations on $V_{1/2}$ of WT and mutant Kv2.2 channels. **C** Statistical analysis showing the effect of the mutations on current density. Data are reported as the mean ± SEM from 5–12 cells. $^{**}P < 0.01$, $^{***}P < 0.001$ *vs* corresponding control.

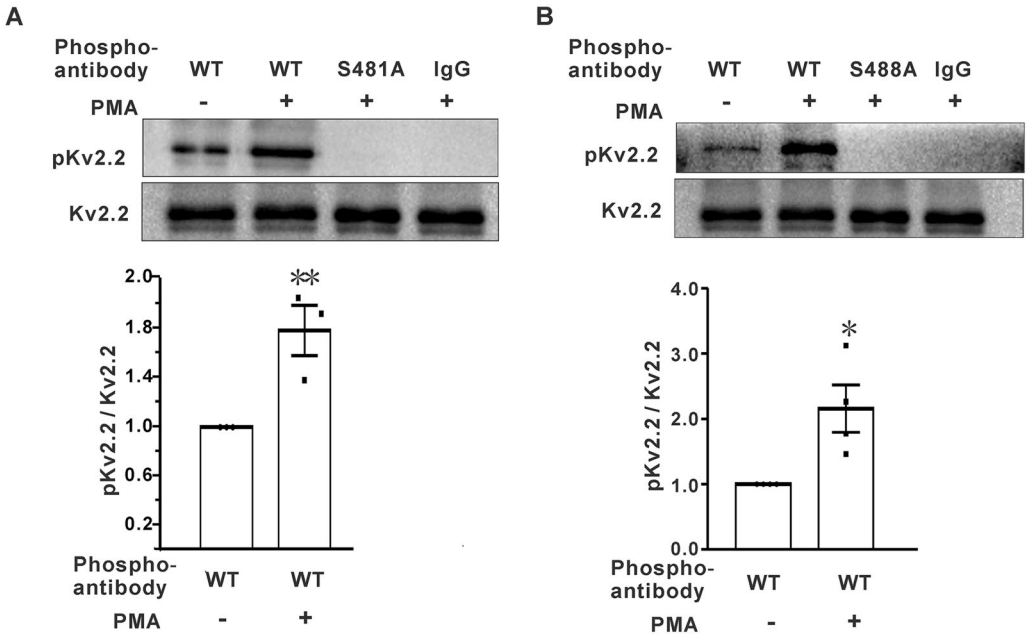

Fig. 7 Phosphorylation state-specific antibodies against S481 and S488 showing the effect of PMA on WT, S481A-. or S488A-mutant Kv2.2 channels in HEK293 cells. **A** Representative Western blots using phosphorylation state-specific antibodies against S481 and statistical analysis showing the effect of PMA on WT Kv2.2 and S481A Kv2.2 channels. **B** Representative Western blots obtained with phosphorylation state-specific antibodies against S488 and statistical analysis showing the effect of PMA on WT and S488A Kv2.2 channels. Data from 3 independent experiments; $^{*}P < 0.05$, $^{**}P < 0.01$ *vs* corresponding control by unpaired *t*-test.

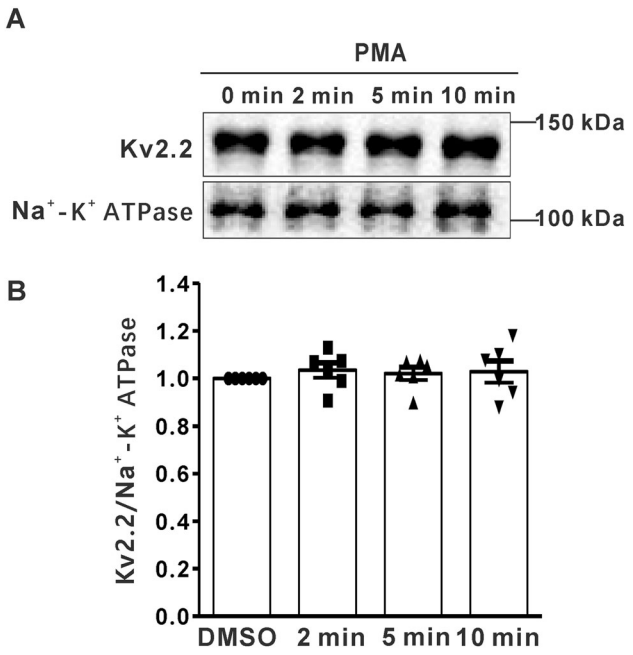

Fig. 8 Effect of PMA on the cell surface expression of Kv2.2 channels in HEK293 cells. **A** Sample images showing the effects of PMA on the cell surface protein expression of Kv2.2. **B** PMA does not alter the cell surface expression of the Kv2.2 channels (n = 6, P >0.05 *vs* corresponding control).

Fig. 9D). PMA did not alter the threshold, height, or width of the APs (Fig. 9E).

In order to test whether the effect of PMA on I_K in cortical pyramidal neurons is mediated *via* its effect on Kv2.2 channels, we selectively inhibited these channels by adding Kv2.2-specific antibodies to the internal solution in the following electrophysiology experiment. The effect of Kv2.2 antibodies was first tested and verified on Kv2.2 channels over-expressed in HEK293 cells. After establishment of the whole-cell configuration, Kv2.2 antibodies gradually inhibited the Kv2.2 current of HEK293 cells until reaching the maximum inhibition of 53.3% ± 3.4% (n = 21, $P = 1.2 \times 10^{-12}$; Fig. 10A). Similarly, intracellular application of Kv2.2 antibodies significantly inhibited the voltage-gated I_K amplitude in pyramidal neurons with maximal inhibition of 60.7% ± 2.4% (n = 6, $P = 1.1 \times 10^{-12}$) and eliminated the PMA-induced inhibitory effect on the I_K amplitude of pyramidal neurons. This inhibition was maintained at 60.4% ± 2.5% and was not significantly different from the inhibition obtained after treatment of neurons with Kv2.2 antibodies (n = 6, $P = 1.1 \times 10^{-12}$; Fig. 10B). Intracellular application of Kv2.2 antibodies mimicked the PMA-induced inhibitory effect on the AP firing frequency in pyramidal neurons (Fig. 10C) and decreased the AP firing frequency by 31.6% ± 3.8% (n = 9, $P = 4.0 \times 10^{-5}$). Moreover, after treatment with Kv2.2 antibodies, PMA no longer exerted its inhibitory effect on AP frequency. The inhibitory effect was maintained at 34.8% ± 3.0%, which was not significantly different from that recorded after Kv2.2 antibody treatment of neurons (n = 9, $P = 1.4 \times 10^{-5}$; Fig. 10C).

Discussion

The phosphorylation-dependent regulation of the Kv2.2 channel has been unclear. In this study, we investigated the mechanism of PKC regulation of Kv2.2 channels and their function. Our results demonstrated that the activity of Kv2.2 channels and their activation gating properties were modified by PKC-dependent phosphorylation of specific S481 and S488 sites, and that PKC controls the excitability of neocortical neurons by phosphorylation of Kv2.2 channels.

Previous studies indicated that the critical difference in primary amino-acid sequences of the Kv2.1 and Kv2.2 channels is located at the proxC sequence in the large cytoplasmic carboxyl-tail region [18, 19, 21]. Temporal restriction of proxC function in Kv2.2 can result from developmentally regulated post-translational modifications of proxC residues, and the primary sequence of proxC has multiple phosphorylation consensus sites including tyrosine kinases, casein kinase 2, and PKC [22, 33]. Phosphoproteomic studies showed that there are five closely situated phosphorylated serine residues (S448, S451, S461, S481, and S488) in the proxC of Kv2.2 [33–37]; and the function of these residues and their phosphorylation-dependent regulation are unknown. By point mutations of the amino-acids from serine to alanine, we demonstrated that the S448A, S451A, and S461A mutations did not alter the effect of PMA on Kv2.2 current amplitude or the shift of the steady-state activation curve. However, individual S481A or S488A mutations partially reduced the effect of PMA on both of these parameters, while double mutation of S481A/S488A eliminated the PMA effects. These data indicate that both S481 and S488 are key amino-acid residues for the PKC-dependent regulation of Kv2.2. Moreover, our data indicated that the effect of PKC on Kv2.2 channels is mainly *via* the PKCδ subtype.

Reversible changes in the phosphorylation state of ion channels usually manifest as changes in the voltage-dependence of channel activation gating kinetics [34]. Kv2.1 is known to be highly phosphorylated under basal conditions. The $V_{1/2}$ in neurons mainly expressing Kv2.1 or in HEK293 cells expressing the Kv2.1 channel can exceed 20 mV [40–42]. Excitatory stimuli or ionomycin-induced dephosphorylation of Kv2.1 lead to a significant hyperpolarizing shift [14, 42]. Relative to the Kv2.1 channel, the Kv2.2 channel is much less phosphorylated

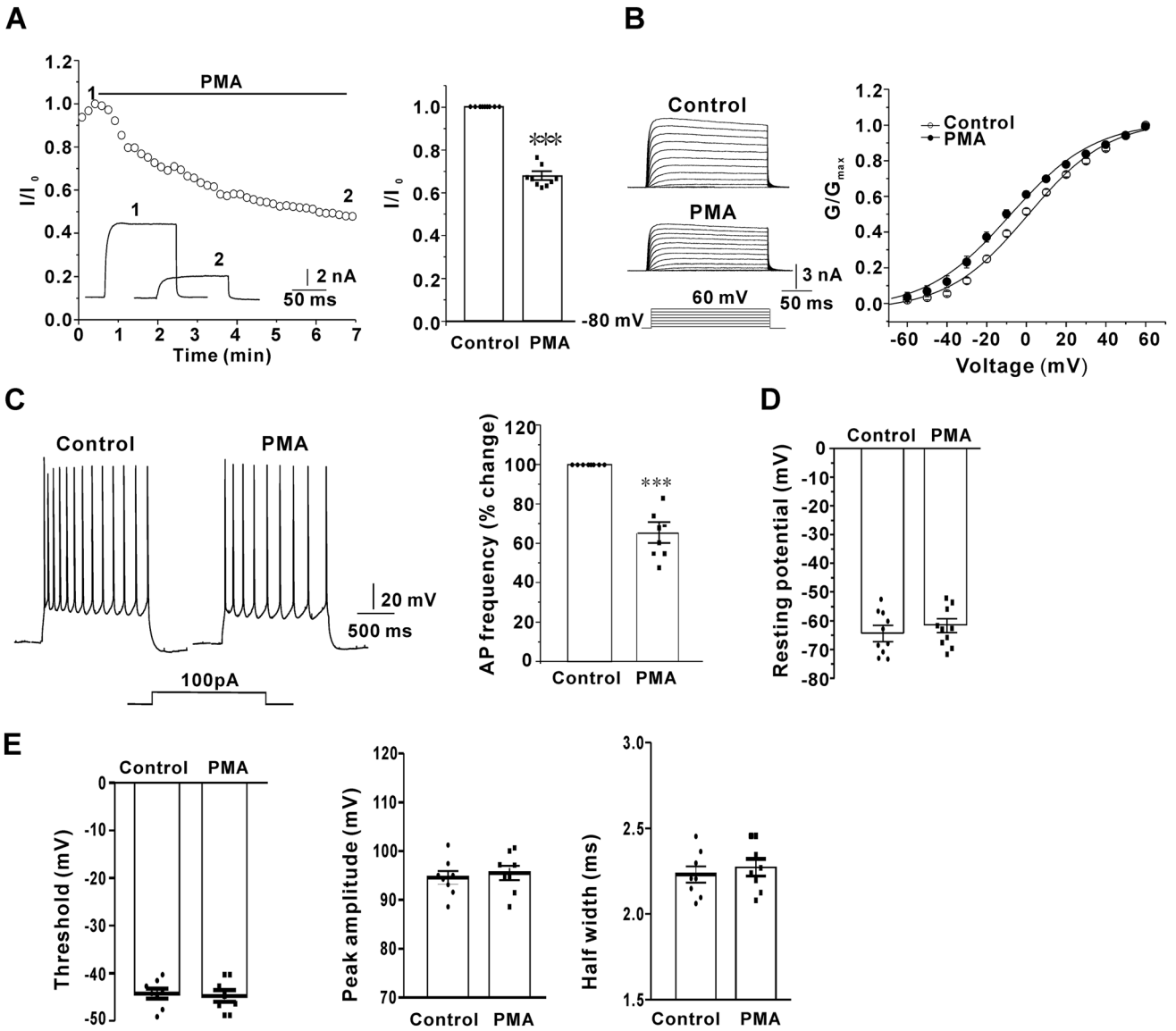

Fig. 9 Effects of PMA on Kv2.2 current amplitude, voltage dependence of activation, and action potentials (APs) in cortical layer II pyramidal neurons in mouse brain slices. **A** Representative time course of the changes in K^+ current amplitudes and statistical analysis showing the effect of PMA on delayed outward rectifier K^+ current. **B** Representative current traces and G–V curves showing the effects of PMA on the voltage-dependence of activation of K^+ currents. **C** Sample recordings of APs and statistical analysis showing the effect of PMA on AP frequency. **D** Statistical analysis showing the effect of PMA on resting potential. **E** PMA does not alter the threshold, height, and width of APs. Data are reported as the mean ± SEM from 6–10 cells. ***P <0.001 *vs* corresponding control by paired *t*-test.

under basal conditions, and its steady-state activation curve is already relatively more hyperpolarized, while the $V_{1/2}$ is close to that of dephosphorylated Kv2.1, so Kv2.2 channels were once considered to be a dephosphorylated version of Kv2.1 channels [2, 22, 23, 30]. In the present study, we were surprised to find that the voltage-dependent activation curve of Kv2.2 channels underlying PKC phosphorylation and the S481D/S488D mutation represented a further hyperpolarizing shift of ~10 mV, instead of the expected depolarizing shift. This is very similar to the shifts caused by enhancing dephosphorylation of the Kv2.1 channel at multiple sites [14, 40]. This result suggested that although Kv2.2 shares some properties with Kv2.1, each channel exhibits intrinsic differences in its voltage-dependent activation properties and phosphorylation-dependent regulation. These differences may be associated with the subtype-specific sequences in proxC or the different phosphorylation sites in the proxC of Kv2.2. Another possibility is that the phosphorylation site modified by PKC in this study (S481/S488) is close to the voltage sensor of Kv2.2. These results indicated that the resemblance in voltage-gating of Kv2.1 and Kv2.2 channels could be

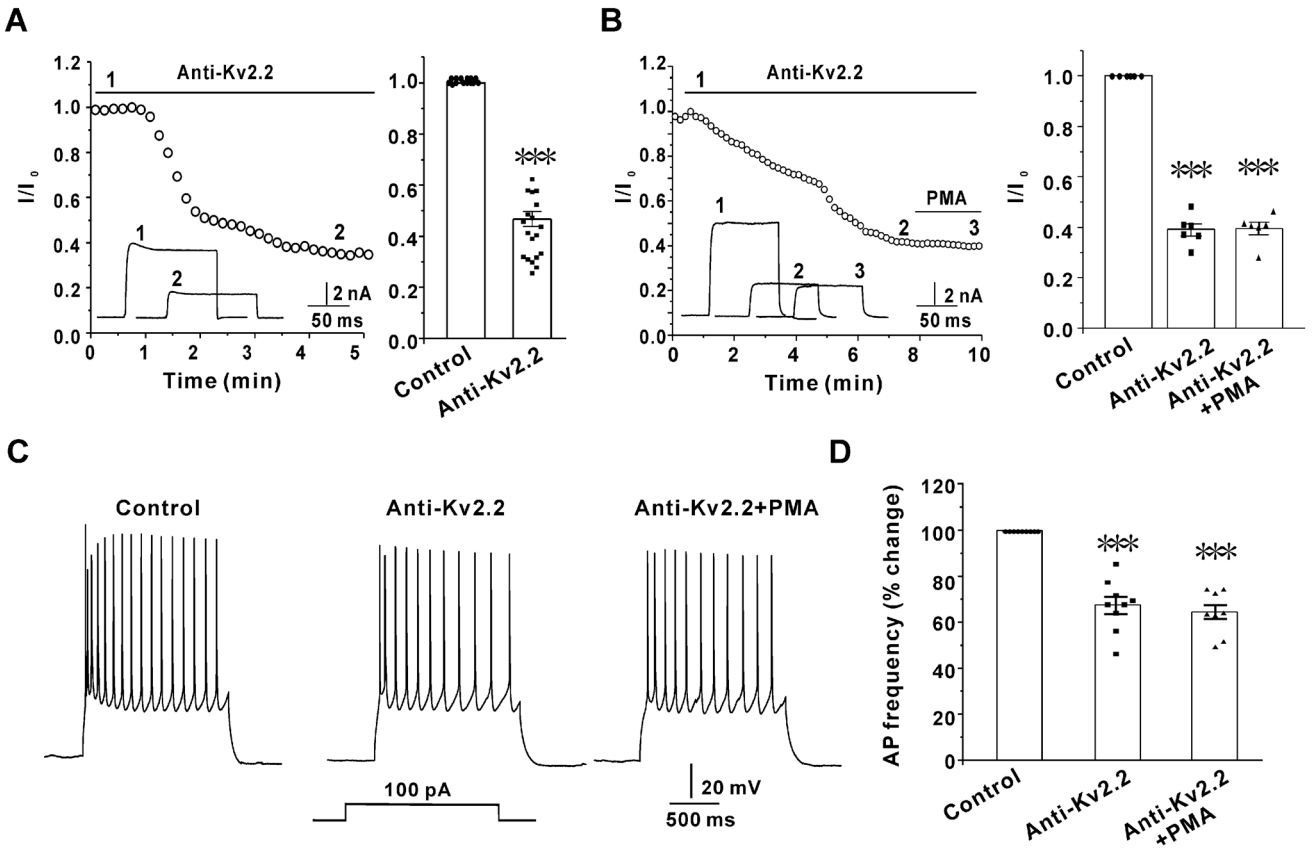

Fig. 10 Effect of Kv2.2 antibody (anti-Kv2.2) on PMA-induced inhibition of Kv2.2 current amplitude and AP frequency in cortical layer II pyramidal neurons in mouse brain slices. **A** Sample recordings and statistical analysis demonstrating the Kv2.2 antibody effect on Kv2.2 channels over-expressed in HEK293 cells (data from cells before and after intracellular dialysis of anti-Kv2.2). **B** Representative time course of the changes in delayed outward rectifier K^+ current and statistical analysis showing the effect of Kv2.2 antibody with/without PMA on this current. **C** Sample recordings and statistical analysis showing the effect of the Kv2.2 antibody with/without PMA on APs. Data are reported as the mean ± SEM from 6–21 cells; ***P <0.001 *vs* corresponding control by unpaired t-test.

obtained *via* parallel and complementary pathways either through enhanced phosphorylation at S481/S488 of Kv2.2 by PKC or reduced phosphorylation at other sites of Kv2.1 by ionomycin or calcineurin [14].

A recent study by Hannah *et al*. showed that Kv2.2 and Kv2.1 have very different expression patterns in the mammalian cortex, and the expression pattern of Kv2.2 does not change to compensate for the loss of Kv2.1 in Kv2.1-knockout mice, which suggests that Kv2.2 and Kv2.1 play independent roles in the mammalian cortex [22]. The study by Hannah *et al*. in mouse cortex further demonstrated that the Kv2.2 channel is the predominant Kv2-family protein in layer II of the mammalian neocortex [22]. Consistent with their results, our Kv2.2 antibody experiments showed that the Kv2.2 channel accounted for almost 60% of the delayed-rectifier K^+ currents in layer II pyramidal neurons in neocortex slices. Similar to the results in HEK-293 cells, activation of PKC by PMA induced a shift of the voltage-dependent activation curve to a more negative potential and decreased the K^+ current amplitude. Moreover, PMA significantly reduced the AP firing rates of layer II pyramidal neurons in neocortex slices. The PMA-induced inhibition of AP frequency was abolished by Kv2.2-specific antibodies. These data are consistent with our previous study [30] and implicated Kv2.2 as the major regulator of excitability in layer II pyramidal neurons of the neocortex, and this can be modulated by PKC-dependent phosphorylation.

In our study, it was evident that Kv2.2-containing channels in layer II pyramidal neurons mediated a delayed rectifier that generated large outward K^+ currents on depolarization. Based on the activation and inactivation kinetics and conductance modeling of the voltage-gated Na^+ and K^+ channels in neurons of the medial nucleus of the trapezoid body, Johnston *et al*. proposed that the Kv2 channel plays a key role in maintaining high-frequency firing by facilitating recovery from the inactivation of voltage-gated Na^+ channels, and thus enhancing AP firing [23]. Kv2.2 facilitation of high-frequency firing has been reported in auditory neurons and mammalian sympathetic

neurons [23, 25]. In addition to the shift of voltage-dependent activation to hyperpolarization potentials, another characteristic of the PKC-dependent regulation of Kv2.2 channels was the significant decrease of current amplitude, which is another common mechanism of ion channel regulation by phosphorylation which changes the number of channels on membranes or alters the conductance of ions through individual channels [34]. The PKC-induced decrease in firing frequency was similar to that induced by the antibody against Kv2.2, suggesting that the inhibition of Kv2.2 current amplitude may be critical in the PKC-dependent regulation of neuronal excitability. However, we noted that the PMA-induced decrease of firing frequency was also very similar to that caused by increasing dephosphorylation of the Kv2.1 channel at multiple sites [14]. Since both the hyperpolarizing shift of the activation curve and reduced Kv2.2 current amplitude induced by PKC were associated with phosphorylation at sites S481/S488, these events may be due to the difference between Kv2.2 and Kv2.1 in the phosphorylation sites in proxC, although this is still a speculation and requires further research.

According to the voltage-dependent activation properties, it may be the case that neurons expressing more Kv2.2 channels have relatively lower intrinsic excitability under basal conditions; here, our data showed that PKC-dependent phosphorylation induced a further lowering of neuronal excitability by altering the activation properties and decreasing the current amplitude. Since phosphorylation in the Kv2.2 basal state is less than in Kv2.1, phosphorylation regulation is more physiological than dephosphorylation regulation for Kv2.2. Our data provide a molecular mechanism for the PKC phosphorylation-dependent regulation of Kv2.2 activity and suggest that any stimulus that activates PKC may regulate Kv2.2, thereby changing neuronal excitability. PKC is not only the downstream signal of G_i protein-coupled receptors but is also the downstream signal of lipid metabolites, intracellular Ca^{2+} activation, and oxidative stress stimulation [43–46], and regulates various neuronal functions [47–49], its effect on Kv2.2 has broad physiological and pathological importance. Accordingly, resveratrol [30] and angiotensin II [7] have been shown to inhibit Kv2.2 by activation of PKC. It may be worthwhile to further investigate whether Kv2.2 is regulated by other protein kinases besides PKC, since a recent study has shown that the phosphorylation levels of serine/threonine of Kv2.2 channels is massively increased in hypertrophic intestinal smooth muscle cells [50].

Acknowledgments This work was supported by the National Natural Science Foundation of China (31771282, and the China Postdoctoral Science Foundation (BX20200093 and 2021M690038).

Conflicts of interest The authors declare that they have no conflict of interest.

References

1. Gutman GA, Chandy KG, Grissmer S, Lazdunski M, McKinnon D, Pardo LA. International Union of Pharmacology. LIII. Nomenclature and molecular relationships of voltage-gated potassium channels. Pharmacol Rev 2005, 57: 473–508.
2. Guan DX, Armstrong WE, Foehring RC. Kv2 channels regulate firing rate in pyramidal neurons from rat sensorimotor cortex. J Physiol 2013, 591: 4807–4825.
3. Liu PW, Bean BP. Kv2 channel regulation of action potential repolarization and firing patterns in superior cervical ganglion neurons and hippocampal CA1 pyramidal neurons. J Neurosci 2014, 34: 4991–5002.
4. Murakoshi H, Trimmer JS. Identification of the Kv2.1 K^+ channel as a major component of the delayed rectifier K^+ current in rat hippocampal neurons. J Neurosci 1999, 19: 1728–1735.
5. Frazzini V, Guarnieri S, Bomba M, Navarra R, Morabito C, Mariggiò MA, *et al*. Altered Kv2.1 functioning promotes increased excitability in hippocampal neurons of an Alzheimer's disease mouse model. Cell Death Dis 2016, 7: e2100.
6. Yu W, Parakramaweera R, Teng S, Gowda M, Sharad Y, Thakker-Varia S, *et al*. Oxidation of KCNB1 potassium channels causes neurotoxicity and cognitive impairment in a mouse model of traumatic brain injury. J Neurosci 2016, 36: 11084–11096.
7. Yeh CY, Bulas AM, Moutal A, Saloman JL, Hartnett KA, Anderson CT, *et al*. Targeting a potassium channel/syntaxin interaction ameliorates cell death in ischemic stroke. J Neurosci 2017, 37: 5648–5658.
8. Pal S, Hartnett KA, Nerbonne JM, Levitan ES, Aizenman E. Mediation of neuronal apoptosis by Kv2.1-encoded potassium channels. J Neurosci 2003, 23: 4798–4802.
9. Tsantoulas C, Zhu L, Yip P, Grist J, Michael GJ, McMahon SB. Kv2 dysfunction after peripheral axotomy enhances sensory neuron responsiveness to sustained input. Exp Neurol 2014, 251: 115–126.
10. Fu JY, Dai XQ, Plummer G, Suzuki K, Bautista A, Githaka JM, *et al*. Kv2.1 clustering contributes to insulin exocytosis and rescues human β-cell dysfunction. Diabetes 2017, 66: 1890–1900.
11. Jacobson DA, Kuznetsov A, Lopez JP, Kash S, Ammälä CE, Philipson LH. Kv2.1 ablation alters glucose-induced islet electrical activity, enhancing insulin secretion. Cell Metab 2007, 6: 229–235.
12. Sesti F. Oxidation of K^+ channels in aging and neurodegeneration. Aging Dis 2016, 7: 130–135.
13. Murakoshi H, Shi G, Scannevin RH, Trimmer JS. Phosphorylation of the Kv2.1 K^+ channel alters voltage-dependent activation. Mol Pharmacol 1997, 52: 821–828.
14. Misonou H, Mohapatra DP, Park EW, Leung V, Zhen DK, Misonou K, *et al*. Regulation of ion channel localization and phosphorylation by neuronal activity. Nat Neurosci 2004, 7: 711–718.
15. Mohapatra DP, Trimmer JS. The Kv2.1 C terminus can autonomously transfer Kv2.1-like phosphorylation-dependent localization, voltage-dependent gating, and muscarinic modulation to diverse Kv channels. J Neurosci 2006, 26: 685–695.
16. Misonou H, Mohapatra DP, Trimmer JS. Kv2.1: a voltage-gated K^+ channel critical to dynamic control of neuronal excitability. Neurotoxicology 2005, 26: 743–752.
17. Misonou H, Mohapatra DP, Menegola M, Trimmer JS. Calcium- and metabolic state-dependent modulation of the voltage-

dependent Kv2.1 channel regulates neuronal excitability in response to ischemia. J Neurosci 2005, 25: 11184–11193.
18. Frech GC, VanDongen AMJ, Schuster G, Brown AM, Joho RH. A novel potassium channel with delayed rectifier properties isolated from rat brain by expression cloning. Nature 1989, 340: 642–645.
19. Hwang PM, Glatt CE, Bredt DS, Yellen G, Snyder SH. A novel K^+ channel with unique localizations in mammalian brain: Molecular cloning and characterization. Neuron 1992, 8: 473–481.
20. Cerda O, Trimmer JS. Activity-dependent phosphorylation of neuronal Kv2.1 potassium channels by CDK5. J Biol Chem 2011, 286: 28738–28748.
21. Trimmer JS, Misonou H. Phosphorylation of voltage-gated ion channels. In: Handbook of Ion Channels. 1st ed. CRC Press, 2015: 531–544.
22. Bishop HI, Guan DX, Bocksteins E, Parajuli LK, Murray KD, Cobb MM, *et al*. Distinct cell- and layer-specific expression patterns and independent regulation of Kv2 channel subtypes in cortical pyramidal neurons. J Neurosci 2015, 35: 14922–14942.
23. Johnston J, Griffin SJ, Baker C, Skrzypiec A, Chernova T, Forsythe ID. Initial segment Kv2.2 channels mediate a slow delayed rectifier and maintain high frequency action potential firing in medial nucleus of the trapezoid body neurons. J Physiol 2008, 586: 3493–3509.
24. Hermanstyne TO, Kihira Y, Misono K, Deitchler A, Yanagawa Y, Misonou H. Immunolocalization of the voltage-gated potassium channel Kv2.2 in GABAergic neurons in the basal forebrain of rats and mice. J Comp Neurol 2010, 518: 4298–4310.
25. Malin SA, Nerbonne JM. Delayed rectifier K^+ currents, IK, are encoded by Kv2 alpha-subunits and regulate tonic firing in mammalian sympathetic neurons. J Neurosci 2002, 22: 10094–10105.
26. Hermanstyne TO, Subedi K, Le WW, Hoffman GE, Meredith AL, Mong JA, *et al*. Kv2.2: a novel molecular target to study the role of basal forebrain GABAergic neurons in the sleep-wake cycle. Sleep 2013, 36: 1839–1848.
27. Tong HX, Kopp-Scheinpflug C, Pilati N, Robinson SW, Sinclair JL, Steinert JR, *et al*. Protection from noise-induced hearing loss by Kv2.2 potassium currents in the central medial olivocochlear system. J Neurosci 2013, 33: 9113–9121.
28. Li XN, Herrington J, Petrov A, Ge L, Eiermann G, Xiong Y, *et al*. The role of voltage-gated potassium channels Kv2.1 and Kv2.2 in the regulation of insulin and somatostatin release from pancreatic islets. J Pharmacol Exp Ther 2013, 344: 407–416.
29. Zhan XQ, He YL, Yao JJ, Zhuang JL, Mei YN. The antidepressant citalopram inhibits delayed rectifier outward K^+ current in mouse cortical neurons. J Neurosci Res 2012, 90: 324–336.
30. Dong WH, Chen JC, He YL, Xu JJ, Mei YA. Resveratrol inhibits Kv2.2 currents through the estrogen receptor GPR30-mediated PKC pathway. Am J Physiol Cell Physiol 2013, 305: C547–C557.
31. Kedei N, Telek A, Michalowski AM, Kraft MB, Li W, Poudel YB, *et al*. Comparison of transcriptional response to phorbol ester, bryostatin 1, and bryostatin analogs in LNCaP and U937 cancer cell lines provides insight into their differential mechanism of action. Biochem Pharmacol 2013, 85: 313–324.
32. Park SK, Hwang YS, Park KK, Park HJ, Seo JY, Chung WY. Kalopanaxsaponin A inhibits PMA-induced invasion by reducing matrix metalloproteinase-9 *via* PI3K/Akt- and PKCdelta-mediated signaling in MCF-7 human breast cancer cells. Carcinogenesis 2009, 30: 1225–1233.
33. Blaine JT, Taylor AD, Ribera AB. Carboxyl tail region of the Kv2.2 subunit mediates novel developmental regulation of channel density. J Neurophysiol 2004, 92: 3446–3454.
34. Cerda O, Cáceres M, Park KS, Leiva-Salcedo E, Romero A, Varela D, *et al*. Casein kinase-mediated phosphorylation of serine 839 is necessary for basolateral localization of the Ca^{2+}-activated non-selective cation channel TR/MIN4. Pflugers Arch 2015, 467: 1723–1732.
35. Huttlin EL, Jedrychowski MP, Elias JE, Goswami T, Rad R, Beausoleil SA, *et al*. A tissue-specific atlas of mouse protein phosphorylation and expression. Cell 2010, 143: 1174–1189.
36. Wiśniewski JR, Nagaraj N, Zougman A, Gnad F, Mann M. Brain phosphoproteome obtained by a FASP-based method reveals plasma membrane protein topology. J Proteome Res 2010, 9: 3280–3289.
37. Trinidad JC, Barkan DT, Gulledge BF, Thalhammer A, Sali A, Schoepfer R, *et al*. Global identification and characterization of both O-GlcNAcylation and phosphorylation at the murine synapse. Mol Cell Proteomics 2012, 11: 215–229.
38. Redman PT, He K, Hartnett KA, Jefferson BS, Hu LD, Rosenberg PA, *et al*. Apoptotic surge of potassium currents is mediated by p38 phosphorylation of Kv2.1. Proc Natl Acad Sci U S A 2007, 104: 3568–3573.
39. Gott AL, Mallon BS, Paton A, Groome N, Rumsby MG. Rat brain glial cells in primary culture and subculture contain the delta, epsilon and zeta subspecies of protein kinase C as well as the conventional subspecies. Neurosci Lett 1994, 171: 117–120.
40. Park KS, Mohapatra DP, Misonou H, Trimmer JS. Graded regulation of the Kv2.1 potassium channel by variable phosphorylation. Science 2006, 313: 976–979.
41. Liu R, Yang G, Zhou MH, He Y, Mei YN, Ding Y. Flotillin-1 downregulates K^+ current by directly coupling with Kv2.1 subunit. Protein Cell 2016, 7: 455–460.
42. Misonou H, Menegola M, Mohapatra DP, Guy LK, Park KS, Trimmer JS. Bidirectional activity-dependent regulation of neuronal ion channel phosphorylation. J Neurosci 2006, 26: 13505–13514.
43. Nishizuka Y. Protein kinase C and lipid signaling for sustained cellular responses. FASEB J 1995, 9: 484–496.
44. Jiang YF, Zhang ZX, Kifor O, Lane CR, Quinn SJ, Bai M. Protein kinase C (PKC) phosphorylation of the Ca^{2+} o-sensing receptor (CaR) modulates functional interaction of G proteins with the CaR cytoplasmic tail. J Biol Chem 2002, 277: 50543–50549.
45. Xu XH, Gera N, Li HY, Yun M, Zhang LY, Wang YH, *et al*. GPCR-mediated PLCβγ/PKCβ/PKD signaling pathway regulates the cofilin phosphatase slingshot 2 in neutrophil chemotaxis. Mol Biol Cell 2015, 26: 874–886.
46. Feng B, Ye WL, Ma LJ, Fang Y, Mei YN, Wei SM. Hydrogen peroxide enhanced Ca^{2+}-activated BK currents and promoted cell injury in human dermal fibroblasts. Life Sci 2012, 90: 424–431.
47. Hirai H. Protein kinase C in the cerebellum: Its significance and remaining conundrums. Cerebellum 2018, 17: 23–27.
48. Hapak SM, Rothlin CV, Ghosh S. aPKC in neuronal differentiation, maturation and function. Neuronal Signal 2019, 3: NS20190019.
49. Callender JA, Newton AC. Conventional protein kinase C in the brain: 40 years later. Neuronal Signal 2017, 1: NS20160005.
50. Liu DH, Huang X, Guo X, Meng XM, Wu YS, Lu HL, *et al*. Voltage dependent potassium channel remodeling in murine intestinal smooth muscle hypertrophy induced by partial obstruction. PLoS One 2014, 9: e86109.